

Recent Results from the Argonne Fragment Mass Analyzer*

C. N. Davids,^(a) B. Back,^(a) I. G. Bearden,^(b) K. Bindra,^{(a),(c)} C. R. Bingham,^(d)
 R. Broda,^{(b),(e)} M. P. Carpenter,^(a) W. Chung,^{(a),(f)} P. J. Daly,^(b) B. Fornal,^(b)
 Z. W. Grabowski,^(b) D. J. Henderson,^(a) R. G. Henry,^(a) R. V. F. Janssens,^(a)
 T. L. Khoo,^(a) T. Lauritsen,^(a) Y. Liang,^(a) R. H. Mayer,^(b) D. M. Moltz,^(g)
 D. Nisius,^(b) A. V. Ramayya,^(c) J. D. Robertson,^(h) F. Scarlassara,⁽ⁱ⁾
 F. Soramel,^{(a),(l)} P. Spolaore,⁽ⁱ⁾ K. S. Toth,^(j) W. B. Walters^(k)

- (a) Argonne National Laboratory, Argonne, IL
 (b) Purdue University, W. Lafayette, IN
 (c) Vanderbilt University, Nashville, TN
 (d) University of Tennessee, Knoxville, TN
 (e) Institute of Nuclear Physics, Cracow, Poland
 (f) University of Notre Dame, South Bend, IN
 (g) Lawrence Berkeley Laboratory, Berkeley, CA
 (h) University of Kentucky, Lexington, KY
 (i) Legnaro National Laboratory, Legnaro, Italy
 (j) Oak Ridge National Laboratory, Oak Ridge, TN
 (k) University of Maryland, College Park, MD

ANL/PHY/CP--78846

DE93 008650

ABSTRACT

The Fragment Mass Analyzer (FMA) at the ATLAS accelerator has been operational for about one year. During that period a number of test runs and experiments have been carried out. The test runs have verified that the ion optics of the FMA are essentially as calculated. A brief facility description is followed by recent experimental results.

1. Introduction

The FMA^{1,2} is an 8.2-meter long triple-focussing recoil mass spectrometer installed at the ATLAS heavy-ion accelerator at Argonne National Laboratory. Figure 1 shows a schematic diagram of the FMA. The FMA separates reaction products from the primary heavy-ion beam and disperses them by M/q at the focal plane. When the FMA is positioned at 0° , the primary beam is stopped on the anode of the first electric dipole, and the two electric dipoles plus the bending magnet constitute an energy-dispersionless mass spectrometer for the reaction products. The two magnetic quadrupole doublets provide geometric focussing and control of M/q dispersion at the focal plane. The FMA has an energy acceptance of $\pm 20\%$, an M/q acceptance of $\pm 4\%$, a maximum solid angle of 8 msr, variable mass dispersion, and an M/q resolution of $>300:1$. The FMA can be

MASTER

The submitted manuscript has been authored by a contractor of the U. S. Government under contract No. W-31-109-ENG-38. Accordingly, the U. S. Government retains a nonexclusive, royalty-free license to publish or reproduce the published form of this contribution, or allow others to do so, for U. S. Government purposes.

ANL-P-20,401

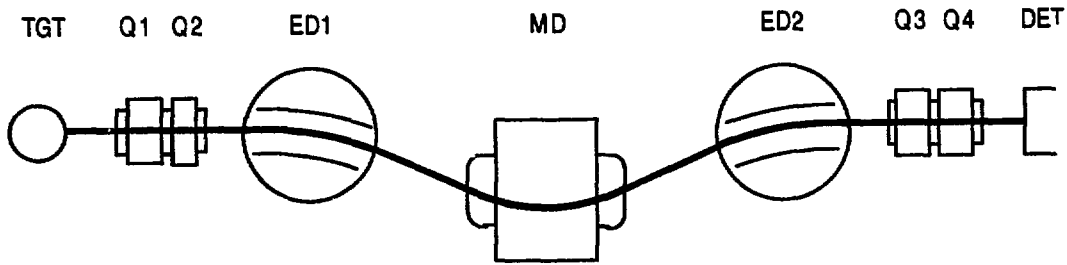


Fig. 1. Schematic diagram of the Fragment Mass Analyzer

positioned at angles between -5° and $+45^\circ$, as well as at distances from the target variable from 10-100 cm in order to accommodate large detector arrays at the target. Figure 2 shows a photograph of the FMA.

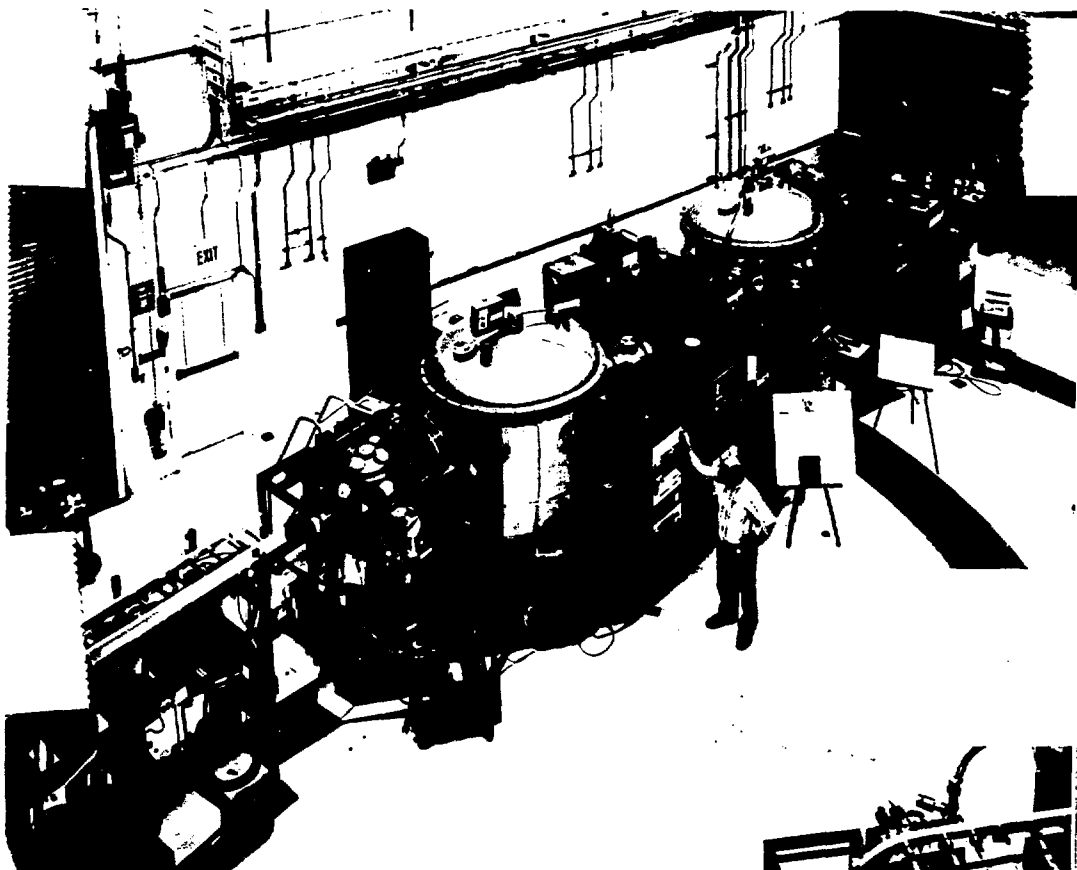


Fig. 2. Photograph of the FMA. The primary beam is incident from the lower left.

2. Experimental Equipment

A number of different experimental systems are available for use with the FMA. Some of these have been constructed by University users.

A 38-cm-diameter sliding-seal scattering chamber is available for use at the target position. It has provision for a target ladder as well as a rotating target wheel used under high beam current conditions. There are two independently controlled rings for mounting detectors, and one side of the chamber has a 30.5 cm by 30.5 cm opening to accommodate an extension for housing large gas detectors. All variable parameters are equipped with stepping motors, controlled manually or by computer. With this scattering chamber in place, the normal distance between the target and the entrance quadrupole is 30 cm. Vacuum is provided by a 1500 l/s cryopump attached to the side of the chamber.

For prompt gamma-ray experiments, an array of ten Compton-suppressed Ge detectors can be placed around the FMA target position. With the full complement of 10 detectors, the distance between the target and the FMA is 35.6 cm. For these experiments the 38-cm scattering chamber is replaced by a 12.1-cm diameter target chamber containing a Si detector beam monitor, a target ladder driven by a stepping motor, and a device to insert thin carbon foils behind the target. These foils are used to reset the charge state of the reaction products following the emission of de-excitation gamma rays.

A 16-segment neutron detector array is available for use at the FMA target position, normally used in conjunction with the Compton-suppressed Ge detectors. It occupies the region between the small target chamber and the entrance to the FMA, so that neutrons evaporated in the forward direction can be detected. In coincidence measurements the neutron array can be used to provide additional information on the Z of the recoils. The detectors utilize pulse shape to discriminate between neutrons and gamma rays at neutron energies above 1 to 2 MeV, and time-of-flight for lower energies.

At the focal plane a 15-cm horizontal by 5-cm vertical parallel-plate avalanche counter (PPAC) is used to measure x- and y-position, time, and energy loss. The PPAC has entrance and exit windows of total thickness 280 $\mu\text{g}/\text{cm}^2$, and uses isobutane gas at a pressure of 3 Torr. Behind it can be placed other detectors such as Si or Bragg curve detectors, or the recoils can be allowed to proceed into other detector systems. A moving tape collector is available for studies of beta activities. A facility to study nuclear moments is under construction behind the FMA. It consists of an array of tilted foils for polarizing the recoils, and a magnet for beta-NMR measurements. Currently under design

is an implantation-decay detection system based on a double-sided Si strip detector with a total of 48×48 pixels.

3. Some Experimental Results

3.1 Yrast Isomers in ^{151}Yb

Recoil ions have transit times through the FMA in the range $0.5\text{--}2 \mu\text{s}$, providing an ideal opportunity to study the decays of microsecond isomers at the focal plane.³ The $^{96}\text{Ru} + 255 \text{ MeV } ^{58}\text{Ni}$ reaction was used to produce fusion products near mass 151 which, after passing through the PPAC, were stopped on a catcher foil placed 10 cm behind the focal plane. Delayed gamma-recoil and gamma-gamma coincidences from the stopped recoils were measured between the PPAC and three gamma detectors. Besides transitions resulting from the decay of the known $N = 82$ isomers $2.6 \mu\text{s } ^{150}\text{Er}$, $0.46 \mu\text{s } ^{151}\text{Tm}$ and $34 \mu\text{s } ^{152}\text{Yb}$, two yrast isomers with half-lives of $20 \pm 1 \mu\text{s}$ and $2.6 \pm 0.7 \mu\text{s}$ were observed in ^{151}Yb . Figure 3 shows the clean separation of transitions feeding and de-exciting the $2.6 \mu\text{s}$ isomer, obtained by sorting the mass-selected gamma-gamma coincidence events using appropriate timing conditions. Further work on these isomers is planned, in particular the observation of conversion electrons using a Si detector.

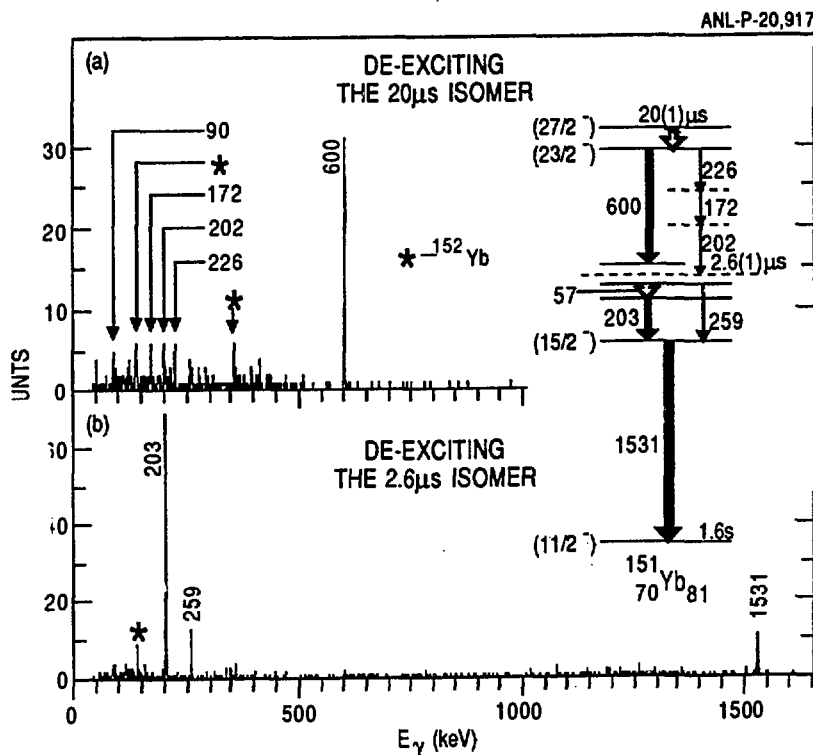


Fig. 3. Gamma rays observed at the FMA focal plane from the decay of high-spin isomers in ^{151}Yb .

3.2 Gamma Spectroscopy of Hg Isotopes

The first gamma-ray spectroscopic studies using the array of ten Compton-suppressed Ge detectors around the FMA target position have been conducted. The reactions $^{155}\text{Gd} + ^{32}\text{S}$ (160 and 190 MeV) and $^{160}\text{Gd} + ^{36}\text{S}$ (157 MeV) were used to produce $^{181-183}\text{Hg}$ and $^{190-192}\text{Hg}$. The FMA transmissions obtained in these runs were 5-10%, with 2 charge states on the focal plane.

In the case of the $^{32}\text{S} + ^{155}\text{Gd}$ reaction, competition between the $4n$ and $p3n$ evaporation channels caused ^{183}Au to be present in the mass 183 spectrum when a charge-state resetting foil was used. When the foil was removed, the relative intensity of ^{183}Au dropped considerably, as is shown in Figure 4. This is due to the presence in the ^{183}Au gamma-ray cascade of one or more transitions with energies < 200 keV having a conversion coefficient of 0.4 or greater. Since the internal conversion process is quite violent, it results in the loss of the emitted electron plus 4-5 outer shell electrons from subsequent Auger transitions. This has the effect of raising the charge state of the Au ions by 5-6 units, thus reducing their transmission to the focal plane since the FMA was set up to transmit only two adjacent charge states.

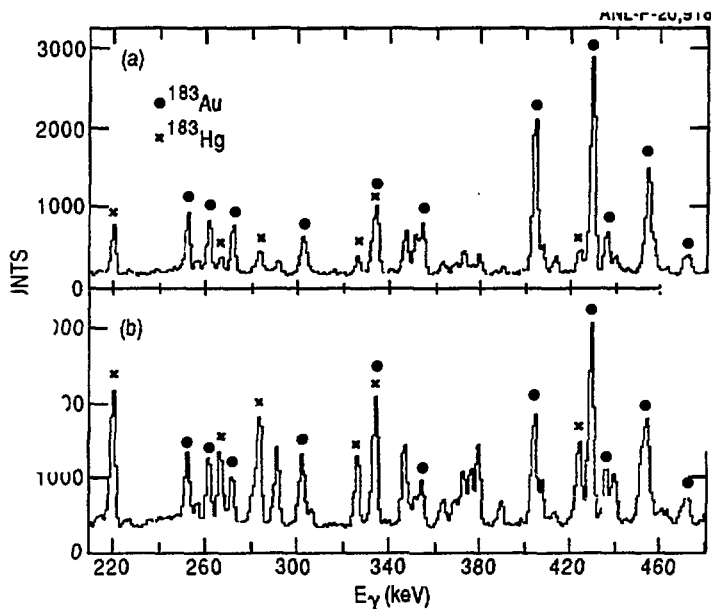


Fig. 4. Prompt gamma rays from 157 MeV $^{32}\text{S} + ^{155}\text{Gd}$ in coincidence with $A = 183$ ions.
a) With a reset foil placed 2 cm behind the target. b) No reset foil used.

In the recoil-gated gamma spectra, transitions of energies 378.1, 418.1, 445.7, and 513.2 keV were assigned to ^{183}Hg and 377.8, 417.5, 445.0, 513.4 were assigned to ^{181}Hg . Analysis of γ - γ - and recoil- γ - γ data is in progress. Many transitions were also seen in ^{182}Hg .

The data for the $^{36}\text{S} + ^{160}\text{Gd}$ reaction demonstrate the sensitivity of the FMA for weak channels. Figure 5 shows how using the mass resolution of the FMA allows one to pull out the gamma rays from the weakly-produced mass 189 channel for analysis of recoil-gamma-gamma coincidences.

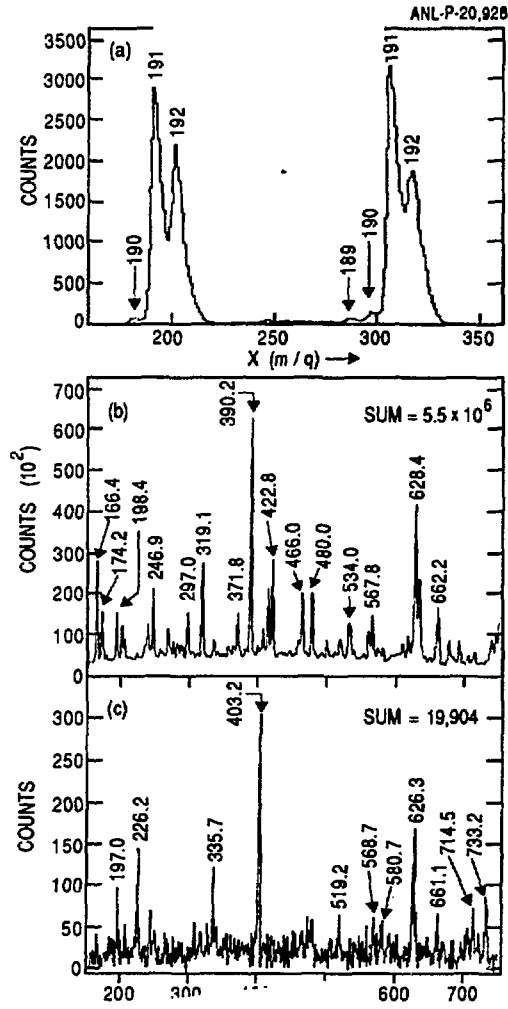


Fig. 5. Results from the $^{36}\text{S} + ^{160}\text{Gd}$ reaction. a) Mass projection showing the low yield of mass 189. b) A portion of the total γ - γ projection of the recoil- γ - γ matrix. Gamma rays from all masses observed in recoil coincidence are present, and the position of the strongest transition in ^{189}Hg at 403 keV is identified. c) A portion of the mass 189-gated γ - γ projection of the recoil- γ - γ matrix.

3.3 Alpha Decay of Neutron-Deficient Pt Isotopes

Early in the commissioning phase of the FMA an experiment was performed to study the decay of short-lived neutron-deficient platinum α -emitting isotopes produced by bombarding ^{144}Sm by ^{32}S . The Pt recoils traversed the FMA, passed through the PPAC at the focal plane and were implanted into a Si(Au) detector placed about 10 cm behind the PPAC. Alpha decay events in the Si detector were counted both during bombardment and beam-off intervals. An electrostatic sweeper was used to prevent the beam from entering the ATLAS accelerator during the beam-off period.

Two different bombarding energies were used: 164 MeV to favor the production of ^{172}Pt and ^{173}Pt , and 200 MeV to favor the production of ^{170}Pt and ^{171}Pt . The half-lives of ^{173}Pt and ^{172}Pt were determined to be 290(60) and 110(20) ms, in agreement with literature values^{4,5}. Figure 6 shows a spectrum accumulated during the beam-off period for the 164 MeV run. Not only are the alphas from $^{171,172,173}\text{Pt}$ present in the spectrum, but also the alphas from their decay daughters as well. Future experiments will continue this work and extend it to other alpha emitters in this mass region.

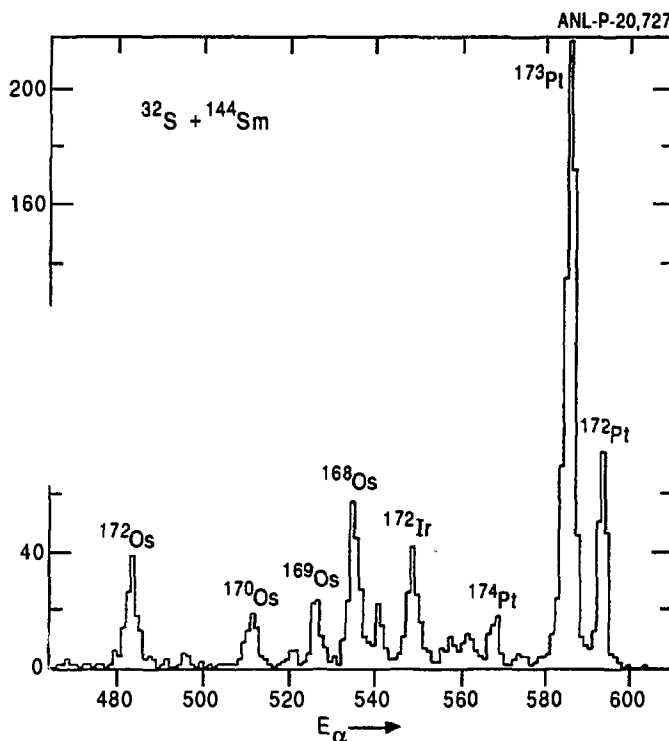


Fig. 6. Alpha-particle spectrum of recoils implanted into a Si(Au) detector behind the FMA focal plane, accumulated during the beam-off interval.

4. Operational Properties of the FMA and Future Plans

The primary beam transmission of the FMA is defined as the intensity of primary beam particles measured on the focal-plane detector divided by the primary beam intensity at the target. The transmission has been measured using a ^{58}Ni beam on a number of targets with masses between 27 and 197. The values ranged from 10^{-6} in the former case to 10^{-11} for the latter. Low primary beam transmissions are obtained by using light beams and heavy targets.

The recoil transmission of the FMA is defined as the number of recoils reaching the focal plane divided by the number of recoils produced at the target, and is highly dependent on a number of variables. First is the FMA's geometric acceptance, typically 5 msr. The transmission also depends on the reaction kinematics and the target thickness, because they determine the angular-, energy-, and charge-state distribution for recoils emerging from the target. Finally, the transmission depends on the M/q of the recoil compared to the central M/q . The transmission of a particular recoil species is measured by observing, in singles and in coincidence with recoils at the focal plane, a particular gamma transition at the target position. The highest transmission measured so far is from a ^{58}Ni on ^{64}Ni experiment. Here a transmission of 24% was measured for the $2p2n$ evaporation product ^{118}Xe . Figure 7 shows the M/q spectrum obtained during that measurement, showing two charge states for $M = 118$ on the focal plane.

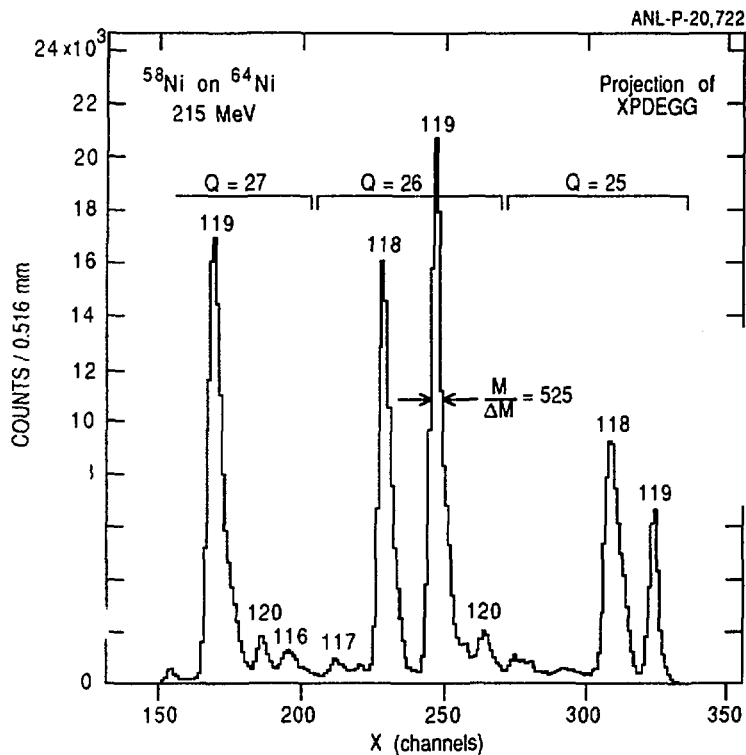


Fig. 7. M/q spectrum at the FMA focal plane from the $^{58}\text{Ni} + ^{64}\text{Ni}$ reaction at 215 MeV.

The mass resolution of the FMA is determined by the beam spot size on target and the angular and energy distributions of the recoils. A circular beam spot size of about 1-mm diameter is used at the FMA target. The highest mass resolution obtained so far with the FMA, 525:1, is shown in Figure 7. In other experiments where the reaction kinematics have been less favorable, mass resolutions of about 350:1 have been obtained.

The FMA has been tested with reactions utilizing both conventional and inverse kinematics. Inverse kinematics has the advantage of high transmission due to forward focussing of the recoils, and high recoil energies which aids in Z-identification. It has the disadvantage of worse primary beam attenuation and large gamma-ray Doppler shifts in at the target.

At present, development work is proceeding on new configurations of detectors for the focal plane, including highly segmented Si detectors for implantation studies and a gas-ionization chamber for Z identification.

References

- * Work supported by the U.S. Department of Energy, Nuclear Physics Division, under contract W-31-109-ENG-38
- 1 C. N. Davids and J. D. Larson, *Nucl. Instrum. Methods* **B40**A1, 1224 (1989).
- 2 C. N. Davids *et al.*, *Nucl. Instrum. Methods* **B70**,358 (1992).
- 3 D. Nisius *et al.*, submitted to *Physical Review C* (1992).
- 4 V. S. Shirley, *Nucl. Data Sheets* **54**, 589 (1988).
- 5 W. Gongqing, *Nucl. Data Sheets* **51**, 577 (1987).

DISCLAIMER

This report was prepared as an account of work sponsored by an agency of the United States Government. Neither the United States Government nor any agency thereof, nor any of their employees, makes any warranty, express or implied, or assumes any legal liability or responsibility for the accuracy, completeness, or usefulness of any information, apparatus, product, or process disclosed, or represents that its use would not infringe privately owned rights. Reference herein to any specific commercial product, process, or service by trade name, trademark, manufacturer, or otherwise does not necessarily constitute or imply its endorsement, recommendation, or favoring by the United States Government or any agency thereof. The views and opinions of authors expressed herein do not necessarily state or reflect those of the United States Government or any agency thereof.